

NASA Technical Memorandum 108833

Experimental/Analytical Approach to Understanding Mistuning in a Transonic Wind Tunnel Compressor

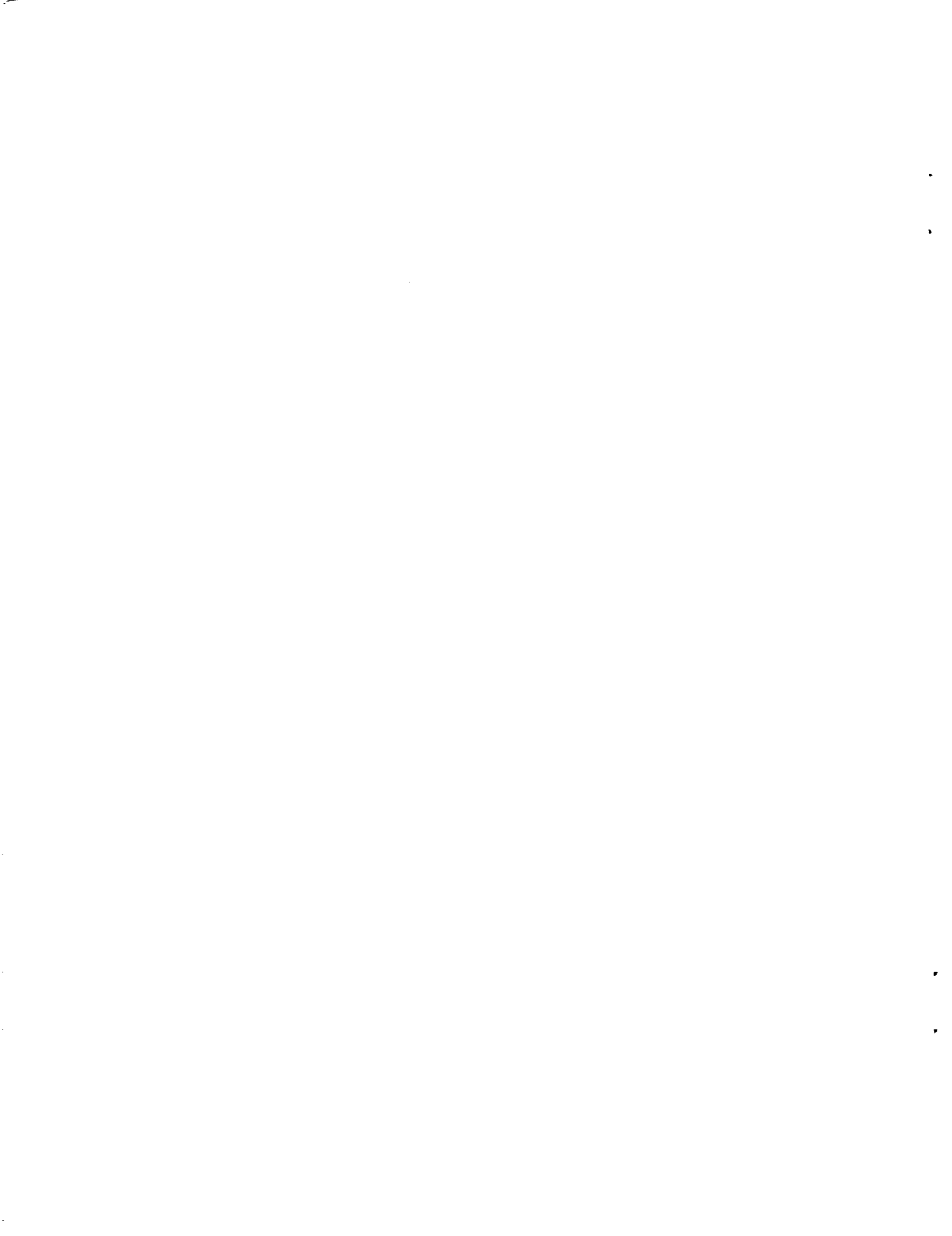
Teri Kaiser, Ames Research Center, Moffett Field, California
Reed S. Hansen, Calspan Corporation, Moffett Field, California
Nhan Nguyen, Ames Research Center, Moffett Field, California
Roy W. Hampton, Ames Research Center, Moffett Field, California
Doug Muzzio, Calspan Corporation, Moffett Field, California
Mladen K. Chargin, Ames Research Center, Moffett Field, California
Roy Guist, Ames Research Center, Moffett Field, California
Ken Hamm, Ames Research Center, Moffett Field, California
Len Walker, Sverdrup Technology, Inc., Moffett Field, California

June 1994



National Aeronautics and
Space Administration

Ames Research Center
Moffett Field, California 94035-1000



Experimental/Analytical Approach to Understanding Mistuning in a Transonic Wind Tunnel Compressor

TERI KAISER, REED S. HANSEN*

NHAN NGUYEN, ROY W. HAMPTON, DOUG MUZZIO,*

MLADEN K. CHARGIN, ROY GUIST, KEN HAMM, LEN WALKER†

NASA Ames Research Center

Introduction

Mistuning is a phenomenon inherent to rotating bladed-disk assemblies. Many such bladed-disk assemblies exist in physical applications such as gas turbines, electric generators, and wind tunnel compressors. Modeling and predictions of how mistuning affects blade vibrations in these compressors is a continuing technical issue which is explored in this study of a large transonic wind tunnel compressor. The authors acknowledge the contributions made to this work by many other unnamed engineers, technicians, and mechanics.

Summary

This paper will briefly set forth some of the basic tenets of mistuned rotating bladed-disk assemblies. The experience with an existing three stage compressor in a transonic wind tunnel will be documented. The manner in which the theoretical properties manifest themselves in this non-ideal compressor will be described. A description of mistuning behaviors that can and cannot be accurately substantiated will be discussed.

Mistuning—What Is Expected

In a nonuniform or mistuned assembly, the blades are not identical, the system characteristics are ill-defined, and the stress distribution is variable and highly uncertain. In a tuned assembly, also referred to as uniform or ideal, the blades are identical, the system characteristics are well defined, and the stress distribution is uniform and predictable.

Any bladed-disk assembly, whether tuned or mistuned, can be characterized by its natural frequencies and corresponding mode shapes. Because of the axisymmetry of both the tuned and mistuned bladed-disk assemblies, the system natural frequencies are seen as pairs of modes (refs. 1–3). These corresponding mode shapes can be defined in terms of nodal diameters and nodal circles. Nodal diameters are diametral lines where a circumferential sine component of the mode shape is at a node, hence a line of nodes appears along a diameter of the assembly. Similarly, nodal circles are radial locations where the radial displacement is at a node and no deflection occurs, thus resulting in concentric circles of nodes. Both shapes are clearly depicted in figures 1 and 2. As will be discussed later, these system modes reflect a combination of both the disc-alone modes and cantilevered blade modes.

In a tuned bladed-disk assembly, the system mode pairs are virtually identical, having the same natural frequency (ref. 3). Their respective mode shapes contain only one diametral, or sine, component (ref. 4). As a result, the tuned system can be precisely quantified both in terms of natural frequencies and mode shapes. Since tuned or ideal systems do not exist in the real world, understanding their behavior is not useful except as a theoretical foundation for mistuned systems. Later, it will be seen how a finite element model's results of an ideal system aided us in identifying the most probable areas of concern for mistuning in an actual system.

Unlike tuned assemblies, mistuned bladed-disk assemblies have system frequency pairs that are no longer identical and corresponding mode shapes that no longer contain a singular diametral component. This deviation in system frequency pairs is often called frequency splitting and is an important characteristic of mistuned systems (refs. 1, 2, and 4). The magnitude of this splitting is not easily quantifiable but is related to the amount of variation in the individual blade frequencies. Frequency splitting not only changes the system natural frequencies by moving them apart, but also changes the

*Calspan Corporation, Moffett Field, California.

†Sverdrup Technology, Inc., Moffett Field, California.

mode shapes corresponding to those frequencies. The resultant modes caused by the splitting of both frequencies and mode shapes are referred to as split modes. The ideal or tuned system can be modeled analytically and the resulting tuned system natural frequencies can be calculated. These natural frequencies can then be used to generate a Campbell plot as seen in figure 3. The natural frequencies are shown by the horizontal lines in the plot.

The spacing of the natural frequencies as seen in figure 3 is indicative of two types of mistuning. The first type of mistuning occurs when the tuned system's natural frequencies are relatively widely spaced (ref. 4). The disc contributes most significantly to these modes. The split modes found in these regions of the Campbell diagram reveal characteristics similar to those of an ideal system, but also show very distinct mistuned features. This type of mistuning is characterized by a resonant condition occurring at one distinct revolution per minute (RPM). The rotor speed at which this resonant response occurs does not vary from blade to blade, but is seen at the same RPM for each blade. This is behavior expected from a tuned system and alone does not qualify it as a mistuned characteristic. When seen in concert with large amplitude variations from blade to blade, it is a mistuned characteristic. Although all blades show their maximum resonant response at the same RPM, the amplitude of those responses may vary by as much as 3 to 1 (ref. 5). This form of mistuning is denoted as Type I.

The second type of mistuning occurs when the tuned system's natural frequencies are quite close (fig. 3). These are modes where the system frequencies are very near the cantilevered blade frequencies. In this condition, the mode pairs split, and the mode shapes begin to overlap and combine with each other in unpredictable ways. It is no longer possible to identify each mode of this system as having "degenerated" from a particular mode of the tuned system. The shapes of these modes tend to be very complex. In fact, these shapes no longer reflect perfectly distinct nodal diameters, but rather show components of almost every diametral order (refs. 1, 2, 4, and 6). This type of mistuning results in the most severe variations in amplitudes. The peak blade stresses may differ by a factor of as much as 10 to 1 (ref. 5). This mistuning is denoted as Type II.

It is important to understand that the potential for exciting any mode increases as the complexity of the modes increases (ref. 2). In order to excite just one component of a system frequency, an input force must be applied that contains the same frequency and shape of that component. To excite an "nth" component of the sys-

tem frequency, the excitation force must appear as an "n" number of sine waves (ref. 3). These sinusoidal disturbances are often induced by obstructions in the air flow of a compressor and can be caused by static structures such as inlet guide vanes, stators, and struts. These cyclic obstructions give rise to circumferential harmonic variations around the compressor and are translated to time varying fluctuations on the bladed-disk as it rotates through the air flow (ref. 3). These disturbances are referred to as n/rev excitations. An "n" number of sine waves are generated when "n" number of evenly spaced disturbances occur for each revolution of the assembly. For example, there are five struts that support our compressor; thus for each revolution, there are five evenly spaced inputs. The struts create a 5/rev excitation and excite modes with a 5 nodal diameter component. As noted previously, each mode contains a component of almost every diametral order, so nearly every mode has the potential to be excited by almost any n/rev excitation. The strength of the response to the n/rev excitation in each case is determined by the magnitude of the n-diameter component in the mode shape. The total response of the system is a combination of all of the system modes being excited by the various n/rev inputs at any given time.

It is helpful to clearly describe the relationships between the system natural frequencies, the rotor speed (in RPM), and the n/rev excitations. For any given rotational speed and n/rev, there is a corresponding frequency, namely $(n/rev) \times (RPM)/(60\text{sec}/\text{min})$. This is the system frequency that will be excited at that load condition. If, for example, the compressor is spinning at 540 RPM, the 5/rev excitation will excite a 45 Hz mode ($5 \times 540/60 = 45$). That is, it will excite the 45 Hz mode if that mode contains a 5 nodal diameter component.

Having an idea of how to recognize the important mistuned characteristics of a bladed-disk assembly, this information may be applied to a particular system in useful and informative ways. Based on this knowledge of mistuned systems, the range of testing possibilities may be narrowed (reducing the time and money spent on testing) and a well-focused empirical search for those mistuned characteristics expected to be found in the non-ideal system may begin. It is desirable to predict those modes that are most likely to be excited and the RPM at which this excitation will occur. To begin, this knowledge is applied to a standard Campbell plot (refs. 4 and 7). It is noted on the Campbell plot shown in figure 3 that in addition to system frequency lines, n/rev lines are drawn that show the expected excitation forces. The critical RPMs, where a system mode is likely to be excited, are found where the system frequencies cross the n/rev lines. Only those system fre-

quencies that contain “n” nodal diameter components will be excited by an n/rev excitation (ref. 8). However, because of mistuning, any mode may potentially be excited by any n/rev excitation because, as mentioned previously, all modes now contain components of nearly every diametral order (refs. 4 and 8).

In addition to finding the critical RPMs at which mistuning would most probably occur, the Campbell plot can also be used to identify the types of mistuning expected. Type I mistuning should occur where the n/rev line crosses system frequencies that are widely spaced and Type II should occur where they are closely spaced (fig. 3). Since Type II mistuning is known to result in more severe stress amplitude variations than Type I, it is normally advisable to thoroughly investigate the regions where Type II mistuning is likely to occur.

Mistuning—What Is Observed

Focus is now shifted from generalized techniques to those used in understanding mistuning in a particular three stage wind tunnel compressor. A careful study of this compressor began only after mistuned properties of the compressor were recognized. When stress data taken from strain gages located on the compressor blades reached values about two times higher than ever previously recorded in the tunnel's 40 year history, interest in understanding mistuning was immediately piqued because these values exceeded the blade allowed endurance limit. These stress variations were not detected in prior tests because minimal data were acquired and analyzed. In order to reconcile the large differences in current versus past data, a much more exhaustive effort was made to explore and document the innate characteristics of this compressor. The results obtained from the investigation reflected both analytical and experimental techniques.

Before proceeding, it is important to note the known sources of excitation in this particular system. The configuration of this three-stage compressor included 5 struts, 34 stators, and 54 inlet guide vanes. These generated 5/rev, 34/rev, and 54/rev excitations. These disturbances also combined to create 10/rev (2 sets of 5 struts), 15/rev, and 20/rev and 68/rev (2 sets of 34 stators) excitations.

In addition to these disturbances exciting the high-order modes, (nodal diameters greater than 26) aliasing also occurred such that mode shapes of lower order were also excited. This aliasing was a result of the differences in the number of blades on a rotor, namely 52, and the number of disturbances. For example, the

54/rev aliased with the 52 compressor blades to excite a two nodal diameter mode (54 inlet guide vanes–52 compressor blades), the 68/rev excited the 16th nodal diameter (2×34 stators–52 compressor blades) and the 34/rev excited the 18 nodal diameter mode (34 stators–52 compressor blades) (ref. 5).

Analytical Evaluation

In order to better understand analytically the phenomena occurring in the compressor, a finite element model of the structure was developed. Because the 52 blades and rotor structure are uniform around the compressor, a cyclic symmetry model of the compressor was used. This form of analysis was advantageous because it minimized computation time by reducing the number of degrees of freedom used in the analysis. In this case, only one blade and 6.92 degrees of the rotor were modeled. In addition, the cyclic symmetry analysis output the system frequencies through harmonics. These harmonics describe the mode shape of a system frequency and simply represent the number of sine waves displaced around the circumference for that system frequency. Harmonics are numerically equivalent to nodal diameters.

The system natural frequencies and mode shapes calculated from the cyclic symmetry finite element model assumed that each of the 52 blades was identical. Clearly then, the finite element model represented the tuned or ideal counterpart of our real compressor and the effects of mistuning were not taken into consideration. Despite the model's simplicity, it was useful in laying the groundwork for more comprehensive investigations and provided a useful starting point for understanding the behavior of the system.

First, to understand the behavior of the disc alone, the frequencies of the compressor with no blades attached to the rotor were calculated. These calculated frequencies are plotted in figure 4. It was noted that with increasing nodal diameters, the system disc frequencies continuously increased. Each of the lines on the plot represented a family of mode shapes which had the same number of nodal circles. Similar to the nodal diameters, the system disc frequencies were found to increase with the increasing number of nodal circles (refs. 1 and 4).

Next, the system frequencies for the bladed-disk were calculated for the first 26 harmonics and plotted against nodal diameter. This plot was used to understand how the disc and blade frequencies combined to form the system mode shapes. It was precisely these system fre-

quencies that were used to generate the Campbell plot shown in figure 3.

When the blades were added to the disc model, the system frequencies no longer increased with increasing nodal diameter, as did the "disc alone" modes but rather began to asymptotically approach the cantilevered blade frequencies. The disc participated in all system modes, but as the number of nodal diameters increased the disc became effectively more stiff and was seen as nearly rigid by the blades (refs. 1 and 4). Overlaying the disc modes onto the system modes plot and noting the cantilevered blade frequencies, it was seen how the disc and blades combined to form the system modes. Figure 5 synthesizes this information in one plot.

The general character of a system mode shape could be determined from its location on the system modes plot. In general, system modes that fall near the disc mode curve (which correspond to the system frequencies on the Campbell plot that are widely spaced) have a larger contribution from the disc and are expected to display Type I characteristics. Those modes that fall near the cantilevered blade frequencies (which correspond to the system frequencies that are closely spaced on the Campbell plot) should have a larger contribution from the blades and typically should yield Type II mistuning.

Using the system frequencies plot in figure 5 with the Campbell plot in figure 3, it could be determined which modes were most likely to be excited and which types of mistuning were to be expected. For compressor rotational speeds of 300–700 RPM, finite element analyses of the tuned system predicted 14 modes that could have been excited by known n/rev excitations. (In figure 5 the RPM ranges are shown by ellipses where the bottom of the ellipse represents 300 RPM and the top represents 700 RPM.) Table 1 shows the 14 modes expected to be seen and the types of mistuning they would display. For example, in the RPM range of interest (300–700) there were five modes that could potentially have been excited by the 54/rev excitation (which excites the two-nodal-diameter modes due to aliasing). Two of these modes (300 Hz and 550 Hz) fell near the cantilevered blade frequencies and were expected to have Type II mistuning. The remaining three two-nodal-diameter modes (380 Hz, 420 Hz and 600 Hz) fell along the curve that was governed by the disc and were expected to result in Type I mistuning. It was interesting to note that the 380 Hz 54/rev mode appeared to be a Type I mode on the system frequencies plot (primarily a disc mode) yet on the Campbell plot it appeared to be very near a Type II mode because of the close spacing of the system frequencies.

Experimental Evaluation

In order to validate the results observed from the analytical model and to understand the stresses observed in the wind tunnel, extensive efforts were made to gather data from the compressor. Various tests were performed both with the compressor stationary (wind off) and with it running (wind on) (ref. 10).

Wind Off Testing

Before examining the behavior of the compressor based on the assumptions made from the analytical analysis, it was necessary to determine how well the calculated system frequencies correlated with measured system frequencies. Modal surveys were performed on the compressor with wind off conditions (ref. 10). To measure the system response, the method employed by Nguyen, et. al. (ref. 10) utilized a shaker located near the outer rim of the third rotor. Fifty-two evenly spaced accelerometers were mounted at three different radial locations, namely, mid-disc, disc rim and blade tip. All blades of the stage were wedged into place in their dovetail sockets in order to simulate the constraints on the blades during compressor operation. Frequency responses were calculated for each measured location. These were then used to determine the system frequencies. In addition, the responses of all 156 locations at a given system frequency were combined to simulate the system mode shape. Figure 6 shows a snapshot of these mode shapes on the experimentally defined model. The number of sine waves (nodal diameters) for that mode were then counted directly from the plots generated by these frequency responses. The measured modes were compared to the calculated modes. The largest system frequency error of 12% occurred at 9 nodal diameters; more typical errors were less than 10%.

Wind On Testing

Equipped with a model that accurately reflected the static wind off system frequencies of the compressor, it was of interest to see if the observed behaviors during operation could be explained. Two types of wind on data are discussed here. The first type represents steady state, constant RPM, or on resonance, data, while the second reviews the transient, variable RPM, or sweep, data (ref. 10).

Wind On—Steady State

To understand the state of stress in the wind tunnel at resonance, a series of tests were performed in which five blades on each of the three stages were gaged. Several different configurations of both bending and torsion strain gages were used. Tests were performed with wind on over a range of 300–700 RPM and at reduced tunnel pressures of 0.5 atmospheres. The speed of the compressor was increased until a resonance was seen on any one of the monitored blades. The tunnel was then held at that RPM until tunnel stability was reached, at which time a data point was taken. For nearly every resonant condition, the RPM at which a specific resonant frequency occurred differed from one blade to the next (as would be expected for Type II mistuning).

To more fully understand what was being measured, the frequency responses of several of these locations were plotted. It was observed that nearly all the resonant frequencies being measured were not single “pure” modes. Frequently, at least two but generally more than two non-uniform peaks were seen grouped closely together. These frequency response plots seemed to indicate a concentration of several system modes within a small frequency range. This verified the existence of Type II modes. The Type I modes that were measured (namely the 600 Hz 54/rev and the 380 Hz 54/rev modes) responded with a the single sharp peak as would be expected from Type I mistuning. It should be noted that although the 380 Hz 54/rev mode showed one very large single peak, there were several additional peaks near that frequency. Figure 7 portrays this but also shows us that these additional peaks were much smaller in magnitude.

Along with the scattering seen in the resonant RPM and system frequencies, variations were also seen in the resonant amplitudes. To expedite the time spent evaluating the variations of all data collected, computer codes were developed that sorted through the entire database of dynamic data. These codes were meticulously calibrated with other commercially available packages to ensure the highest data quality. All critical data were verified using three or four comparable techniques and any discrepancies were documented and understood. One set of computer codes synopsised the data by looking only for significant responses, and then presenting those responses sorted by either amplitude, frequency, RPM, or n/rev.

A technique that was especially helpful was sorting the responses by n/rev excitation. These n/rev excitation forces were calculated for all frequencies in the

frequency response based on the RPM at which the data was taken. Once all of these excitation forces were calculated, the data were sorted by the n/rev excitations. This provided a cleaner examination of the system frequencies by limiting the investigation to the contributions of only one excitation at a time. Figure 8 is a series of plots of amplitude versus frequency for each of the dominant n/rev excitations and shows how the system responded to that excitation for all of the RPM measured. Table 1 showed minimal scatter for Type I modes (380 Hz 54/rev; 420 Hz 54/rev and 600 Hz 54/rev). For the remaining modes measured, the scatter was as much as 19 RPM. As expected for Type II modes, many of the n/rev excitations displayed modes that appeared to be multiple modes with several peaks closely spaced.

When looking at the modes where Type I mistuning was expected (such as the 380 Hz 54/rev mode) the resonant amplitudes were seen to vary by factors of as much as 2 to 1 (table 1). For Type II mistuned modes (like the 300 Hz 34/rev mode) the amplitudes varied from one blade and location combination to another comparable blade and location by as much as 5.28 times on one rotor.

It is noted here that several different techniques may be used to obtain representative stress amplitude ratios from the very large quantity of data available to us. The amplitudes mentioned here and shown in Table 1 do not reflect the largest amplitude ratios possible. To obtain the maximum amplitude ratio, which would represent the full spectrum of possibilities, we would take the lowest stress amplitude of any strain gage, at a particular location on any blade, and compare it to the largest amplitude obtained from any other strain gage at the same location on another blade. Of course these amplitudes could only be compared if they were taken from blades on the same rotor and at the same tunnel conditions.

The ratios presented here, however, represent a much more conservative approach. Instead of comparing minimums to maximums, each gage’s output was searched throughout all measurements taken in the RPM range of interest. Each gage’s largest response was saved for that RPM range for comparison with other gages. Only gages at the same location on different blades were compared against each other to avoid worrying about modal participation factors (MPF). However, it should be noted in passing that when a strain gage with a very low response to a mode is used to study that mode, variable stress amplitudes may occur from one blade to another due to the influence of other active modes upon the measured strain.

Data in table 1 where the MPF of the primary mode was low are flagged. To obtain the data in table 1, all gages at the same location on different blades were compared for all data points taken over a specified RPM range. These maximal values were then compared to each other to obtain the largest ratio, and those are the ratios reported.

It was interesting to observe the large number of n/rev excitations that comprised a resonant condition. Several "odd" excitations, such as a 29/rev, were found to contribute significantly to the overall frequency response. Additionally some n/rev excitations that were expected to be seen were not. This confirmed the complexity of measuring the mode shapes of a mistuned system.

It should be noted that measurements were also made in the attempt to calculate system damping for possible use in frequency response analysis of the finite element model. Since there were few published reports on the effects of mistuning on the system's damping, there were no guidelines for the data that was to be observed. However, like the system frequencies, amplitudes, and RPM, the damping values also varied significantly from one measurement condition to the next for any given system frequency. Though a small amount of the variation in the damping values obtained could have been attributed to the method of calculation, the amount of damping scatter observed was well beyond computational or systematic errors. These variations served as another validation of the severity of mistuning in this system.

Wind On—Transient

After completing the steady state wind on testing, a series of sweep tests were performed (ref. 10). Measurements were again taken on all three rotors of the compressor, but with a different set of instrumented blades installed in all three rotors. Five adjacent blades on each of the three stages were again gaged with both bending and torsion strain gages. The tunnel was held at constant pressure and the compressor was run through various RPM ranges. The average rate of the sweeping was a little greater than one RPM/sec.

Data from these sweeps were used to generate waterfall plots or three-dimensional Campbell plots. Figures 9(a) and 9(b) show two typical waterfall plots. These plots were extremely useful in giving an overall understanding of the behavior of the compressor for the various RPM ranges measured. The n/rev lines were seen as the diagonal lines across the plots, while the vertical lines represented the system frequencies. As expected, the 34/rev, 54/rev, and 68/rev were seen very

clearly on all the plots. It was interesting to note on various plots additional n/rev lines that were not expected such as the 88/rev and the 102/rev.

As with the prior data, amplitude scatter was observed in all modes. The smallest ratio of maximum resonant stress amplitude to minimum resonant stress amplitude was found to be 1.67 for the mode at 50 Hz which was excited by the 10/rev. The largest amplitude ratio of 4.90 was at 550 Hz and was excited by the 68/rev excitation.

The analysis of the sweep data revealed that the RPM at which resonance occurred tended to follow the same trends as those observed in the steady state condition. True to theory, the Type II modes experienced much larger RPM scatter than did the Type I modes. It was interesting to observe the many individual peaks closely spaced in frequency as the n/rev line cut through those frequencies. These peaks along an n/rev line resembled the teeth on a comb.

Discussions

It is of interest to pass on some important lessons learned about studying mistuning in a wind tunnel's three-stage compressor. Every subject that participated in this engineering assessment cannot be addressed. Several subjects believed to be helpful to those with similar facilities will be addressed cursorily.

The computer codes discussed previously provided the ability to scale data taken at different pressures to a maximum expected pressure so that all data could be evaluated comparably. However, after data were taken directly at different pressures, it was discovered that the equations that had traditionally been used to perform pressure scaling on the data were largely inadequate. Because of this, no scaling equations were used and only data taken at the same pressure were compared.

The computer codes also provided scaling factors that predicted peak stresses on a blade by multiplying the response at a given measurement location by an appropriate participation factor. These MPFs or scaling factors were based on the cantilevered blade frequencies and mode shapes calculated from a finite element model of the cantilevered blade (ref. 10). It was discovered that when scale factors of less than one tenth were used, the predicted stresses were unrealistically high. The use of MPFs was discontinued in our study because it was believed that they did not accurately reflect the behavior of the system.

A theoretical analysis was also performed to predict the relationship between transient and steady state wind on

data (ref. 9). As a result of this analysis, it was expected that the transient response would be less than the steady state response. This seemed to be an intuitively correct assumption, because as the compressor swept through the RPM range, the system had no time to build up to a fully resonant condition. Contrary to our beliefs, actual measurements sometimes gave higher values for most modes in transient tests than in steady state tests. This was puzzling, but when thought about in terms of mistuning it makes some sense. The analyzed sample length of the steady state data was about four seconds at a specific RPM plus or minus two tenths of an RPM. There is no guarantee of having sensed the aggregate resonance of each rotor's 52 blades at that specific RPM. Nor is there assurance of capturing it at the next highest RPM, or the one thereafter. In fact, for those four seconds the aggregate resonant RPM may have changed and probably was not at the exact RPM chosen as the RPM setpoint. On the other hand, if during that same four second period the compressor swept through each and every RPM or fraction thereof across a seven RPM range, the chances of capturing the aggregate resonant RPM increased dramatically. Thus, on closer examination, sweeping through a range of RPMs could yield larger peak stresses than discrete steady state measurements if the latter data did not precisely capture the peak resonance.

There was some concern with respect to the repeatability of the measurements. Specifically, the stress amplitudes were compared for runs where the RPM and pressure settings were the same to within one tenth of an RPM and 0.003 atm. For the measurements being compared, the strain gage locations were unaltered. Stress amplitudes on the same gage were found to vary by as much as 30% from one run to the next. It is believed that these large variations in amplitude are due to the complexity of the mode shapes which result from the mistuning in the system. Predicting the maximum stress amplitude for a given blade was very difficult even when large quantities of data were taken.

The finite element analyses performed were helpful in identifying those modes that were most likely to experience large amounts of mistuning. These predictions correlated remarkably well with results obtained from testing. Unfortunately, they were not able to answer the most critical questions such as: What was the maximum stress expected for a mistuned mode or Which blade would 'see' the largest stress?

Because accurate forcing function and system damping values were unavailable, the analytical model was unable to give any indication of what the maximum stress amplitude for any mode would be. Testing gave actual numbers that could be used to obtain a better overall idea of the tunnel's stress profile. Using those measurements, the modes of most concern were identified and efforts were focused on minimizing their stress. Unfortunately, it could not be verified that the peak stress had been measured even after significant testing and analysis of the results. Using the measured stresses and our knowledge of mistuning, conservative estimates of the possible magnitude of the unmeasured peak dynamic stresses were made for assessing the risk of exceeding the blade's fatigue strength.

Conclusions

Mistuning can be a very challenging problem to quantify. Our goal in this effort was to better understand mistuning, and its various manifestations in this compressor, as well as define the probable maximum stresses the rotor blades would see. Because of the very costly nature of gaging every blade, it was desirable to obtain realistic predictions of maximum stress amplitudes from the data collected by relatively few gaged blades. Analytical and experimental modal analyses of the entire compressor enabled us to identify with certainty the types of modes indigenous to this compressor, their frequencies, and the corresponding number of nodal diameters. With this information, the defining ovals seen in figure 5 were drawn and estimates of the types of mistuning associated with each and every measured mode were established. The waterfall plots from experimental wind on testing were helpful in identifying which of the many possible modes had significant stress amplitude. The variance in these amplitudes (i.e., their ratios) confirmed the types of mistuning predicted for them. With this information, mistuning factors could be applied to estimate peak blade stresses over the tunnel's entire operating range. Prudence requires that these estimates be made as conservatively as practicable due to the catastrophic consequences that can occur from underestimating mistuning in compressors.

References

1. D. J. Ewins: Structural Dynamic Characteristics of Bladed Assemblies. AGARD Manual on Aeroelasticity in Axial-Flow Turbomachines, X AGARD-AG-298, vol. 2, 1973, pp. 15.1–15.35.
2. D. J. Ewins: Vibration Modes of Mistuned Bladed Disk. *J. of Engineering for Power*, July 1976, pp. 349–355.
3. D. J. Ewins: A Study of Resonance Coincidence in Bladed Discs. *J. Mech. Engineering Science*, vol. 12, no. 5, 1970, pp. 305–312.
4. D. J. Ewins: Vibration Characteristics of Bladed Disc Assemblies. *J. Mech. Engineering Science*, vol. 15, no. 3, 1973, pp. 165–185.
5. D. J. Ewins: Personal Contact, Department of Mechanical Engineering, Imperial College of Science and Technology, London, England, 1993–1994.
6. A. V. Srinivasan, H. M. Frye: Effects of Mistuning on Resonant Stresses of Turbine Blades. *Structural Dynamic Aspects of Bladed Disk Assemblies*, 1976, pp. 57–71.
7. W. Campbell: The Protection of Steam-Turbine Disk Wheels from Axial Vibration. *Amer. Soc. of Mech. Engineers*, May 1924.
8. L. E. El-Bayoumy, A. V. Srinivasan: Influence of Mistuning on Rotor-Blade Vibrations. *AIAA J.*, vol. 13, no. 4, 1975, pp. 460–464.
9. M. Chargin: Vibration During Acceleration Through Critical Speed. NASA Ames Research Center Internal Memo, 1993.
10. N. Nguyen, D. Muzzio, R. Guist, R. Hansen: Experimental Investigation of the Rotor Blade Vibration in the Three Stage Compressor of the 11-Foot Transonic Wind Tunnel. To be published as a NASA Technical Memorandum.

Table 1. "Wind On" Results.

| Freq. (Hz.) | N/Rev | Rpm | Mistuning Type | Steady State | | Sweep | |
|----------------|-------|-----|-------------------|--------------------|----------------|--------------------|----------------|
| | | | | Amplitude Ratio | Rpm Scatter | Amplitude Ratio | Rpm Scatter |
| 50 | 10 | 300 | Type II | 1.27 | 15 | 2.00 | 16 |
| 160 | 15 | 640 | Type II | 4.19 | 19 | 3.51 | 67 |
| 160 | 20 | 480 | Type II | 1.65 | 7 | 4.24 | 30 |
| 240 | 34 | 425 | Type II | 2.64 | 6 | * | * |
| 300 | 34 | 530 | Type II | 4.76 † | 11 | 2.79 | 21 |
| 380 | 34 | 670 | Type II | 3.50 | 10 | * | * |
| 300 | 54 | 330 | Type II | 3.19 † | 5 | 4.42 | 8 |
| 380 | 54 | 420 | Type I | 2.05 | 1 | 4.32 | 3 |
| 420 | 54 | 465 | Type I | 1.21 | 1 | * | * |
| 550 | 54 | 610 | Type II | 2.87 | 10 | 3.39 | 21 |
| 600 | 54 | 665 | Type I | 1.34 | 0 | * | * |
| 380 | 68 | 335 | Type II | 2.88 | 10 | 3.88 | 14 |
| 550 | 68 | 485 | Type II | * | * | 4.90 | 18 |
| 700 | 68 | 620 | Type II | 5.28 | 10 | 2.78 | 17 |

*Insufficient data

† Modes measured by gages with low modal participation factors



Figure 1. (a) 2 Nodal diameters, (b) 3 nodal diameters.

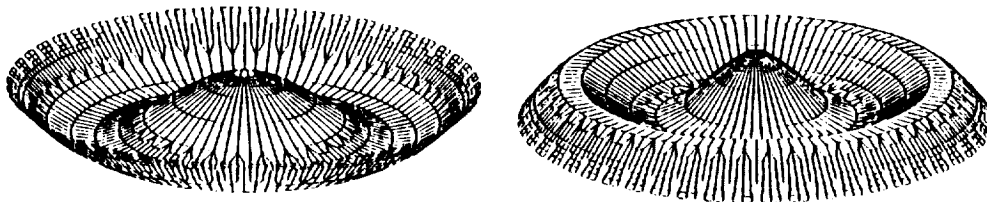


Figure 2. (a) 2 nodal circles, (b) 3 nodal circles.

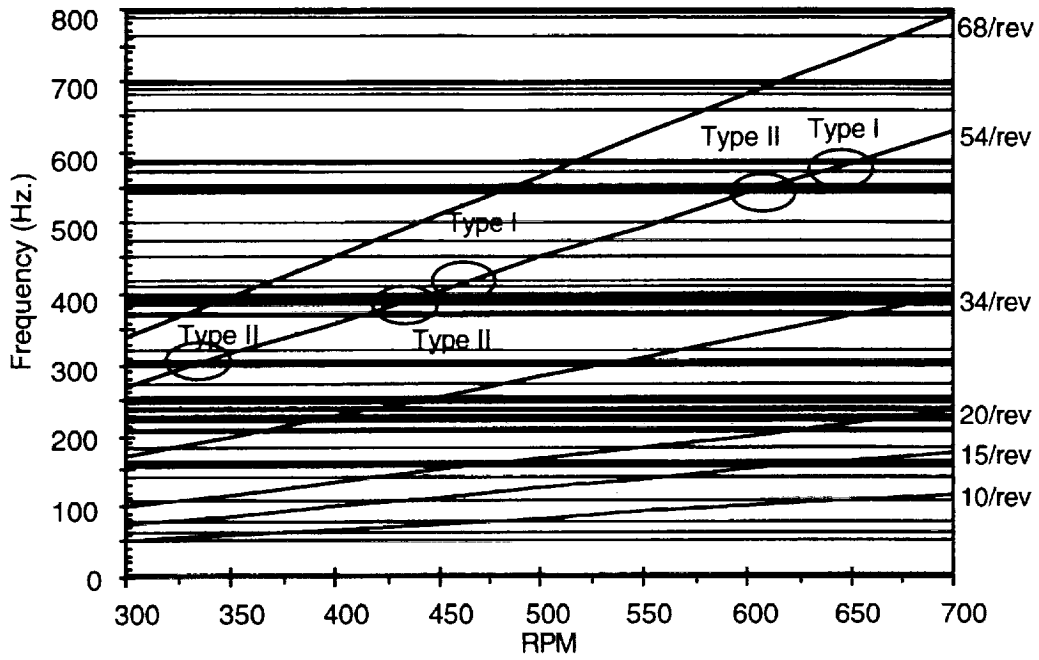


Figure 3. Campbell plot.

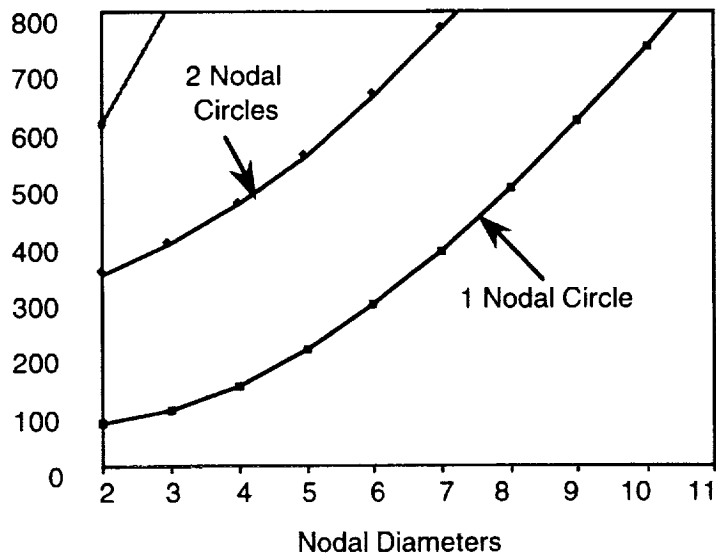


Figure 4. Disc alone frequencies.

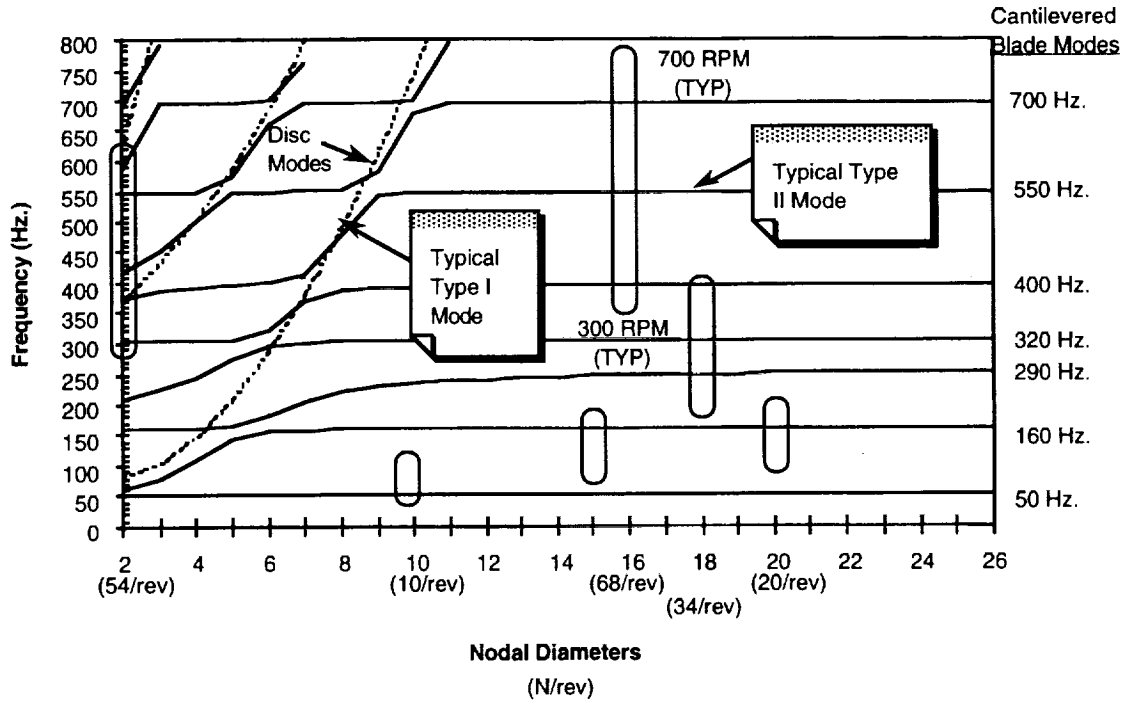


Figure 5. System frequencies.

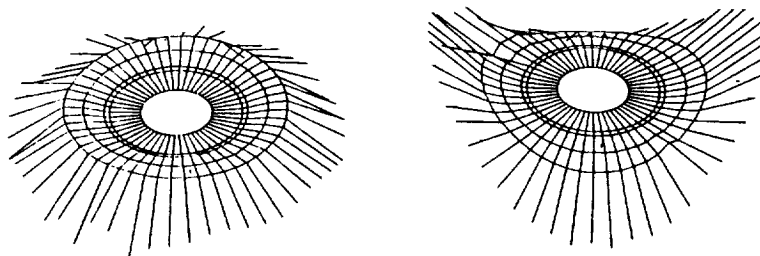


Figure 6. (a) 1 nodal circle, (b) 2 nodal diameters.

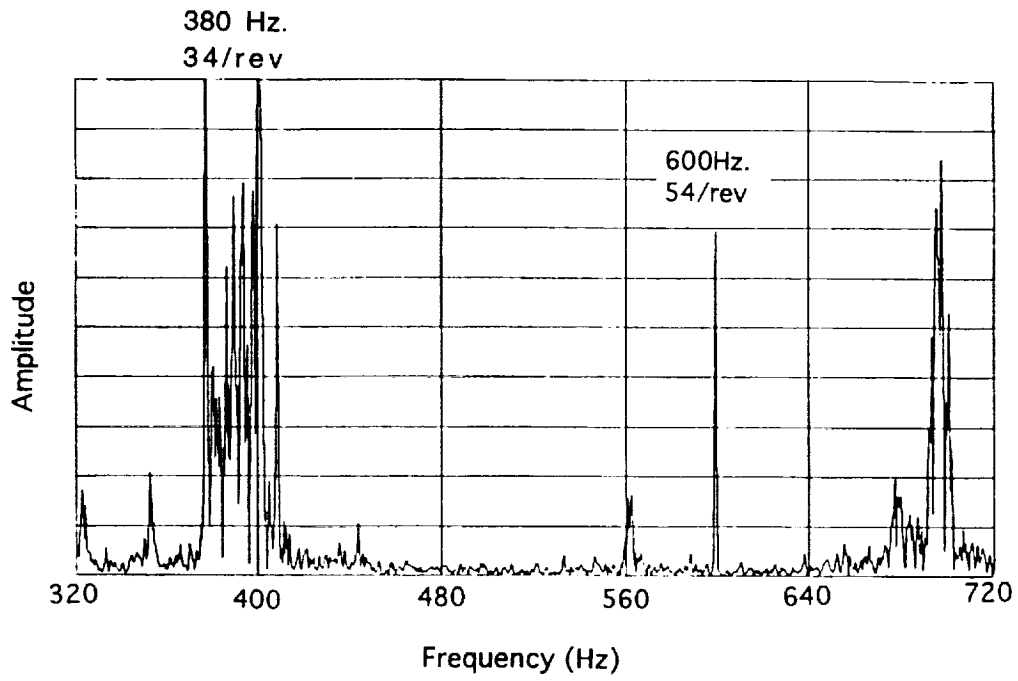


Figure 7. "Wind On" steady state frequency response.

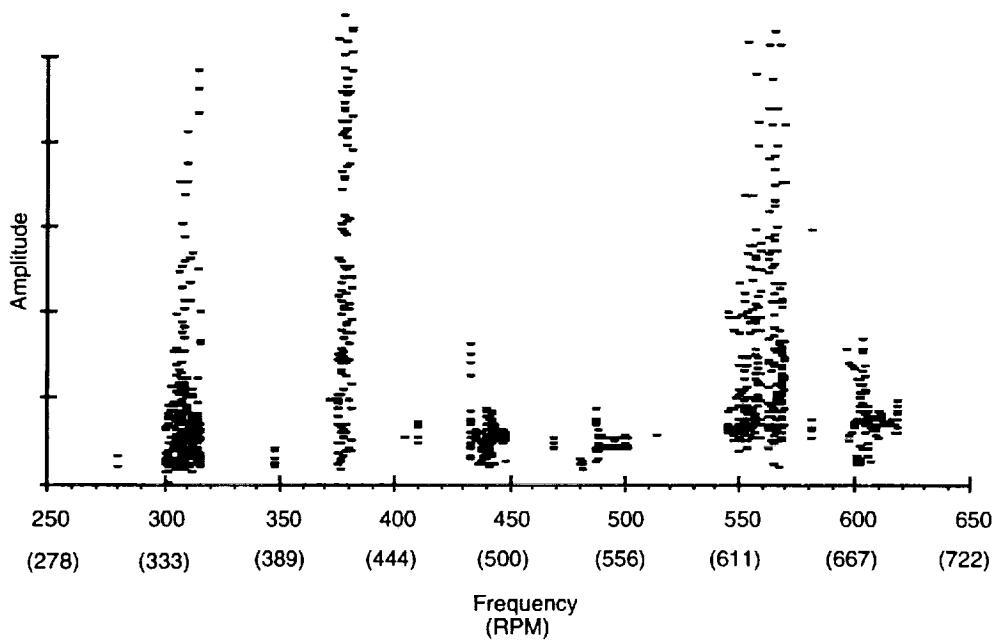


Figure 8. Response due to 54/rev excitation.

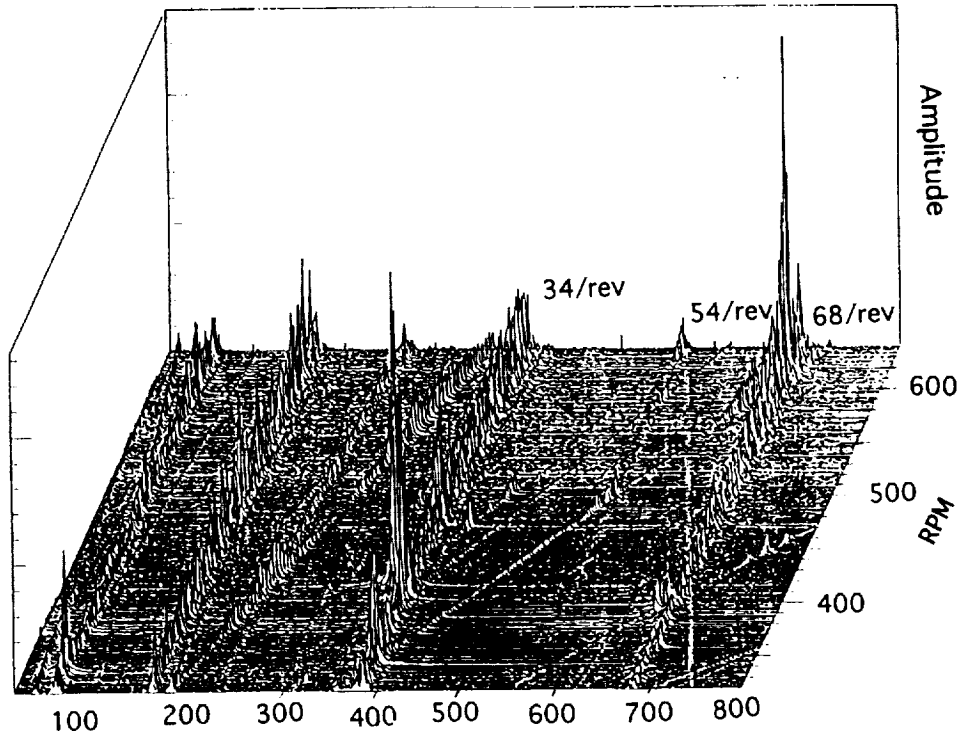


Figure 9. (a) "Wind On" transient "Waterfall plot"-bending gage.

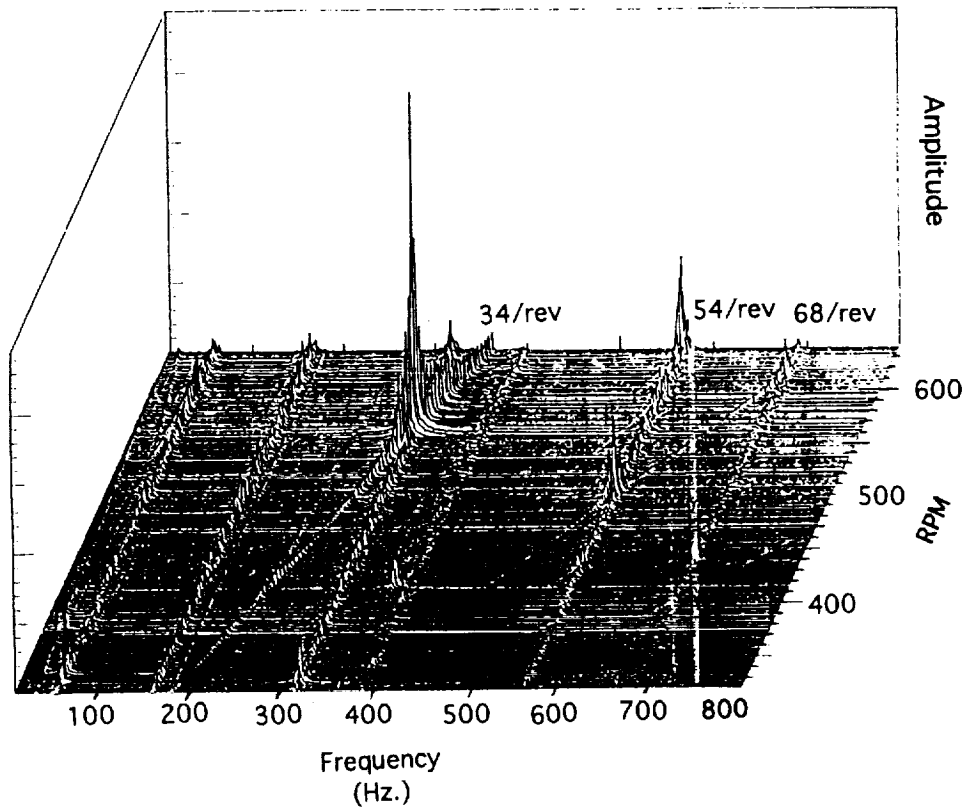


Figure 9. (b) "Wind On" transient "Waterfall plot"-torsion gage.

REPORT DOCUMENTATION PAGE

Form Approved
OMB No. 0704-0188

Public reporting burden for this collection of information is estimated to average 1 hour per response, including the time for reviewing instructions, searching existing data sources, gathering and maintaining the data needed, and completing and reviewing the collection of information. Send comments regarding this burden estimate or any other aspect of this collection of information, including suggestions for reducing this burden, to Washington Headquarters Services, Directorate for Information Operations and Reports, 1215 Jefferson Davis Highway, Suite 1204, Arlington, VA 22202-4302, and to the Office of Management and Budget, Paperwork Reduction Project (0704-0188), Washington, DC 20503.

| | | | |
|---|---|---|-----------------------------------|
| 1. AGENCY USE ONLY (Leave blank) | 2. REPORT DATE June 1994 | 3. REPORT TYPE AND DATES COVERED Technical Memorandum | |
| 4. TITLE AND SUBTITLE Experimental/Analytical Approach to Understanding Mistuning in a Transonic Wind Tunnel Compressor | | 5. FUNDING NUMBERS Program Code 977-4203 | |
| 6. AUTHOR(S) Teri Kaiser, Reed Hansen,* Nhan Nguyen, Roy W. Hampton, Doug Muzzio,* Mladen K. Chargin, Roy Guist, Ken Hamm, and Len Walker† | | 8. PERFORMING ORGANIZATION REPORT NUMBER A-94104 | |
| 7. PERFORMING ORGANIZATION NAME(S) AND ADDRESS(ES) Ames Research Center Moffett Field, CA 94035-1000 | | 10. SPONSORING/MONITORING AGENCY REPORT NUMBER NASA TM-108833 | |
| 9. SPONSORING/MONITORING AGENCY NAME(S) AND ADDRESS(ES) National Aeronautics and Space Administration Washington, DC 20546-0001 | | 11. SUPPLEMENTARY NOTES Point of Contact: Teri Kaiser, Ames Research Center, MS 213-3, Moffett Field, CA 94035-1000; (415) 604-4094 *Calspan Corporation, Moffett Field, California 94035; †Sverdrup Technology, Inc. Moffett, California 94035 | |
| 12a. DISTRIBUTION/AVAILABILITY STATEMENT Unclassified — Unlimited Subject Category 39 | | 12b. DISTRIBUTION CODE | |
| 13. ABSTRACT (Maximum 200 words) This paper will briefly set forth some of the basic tenets of mistuned rotating bladed-disk assemblies. The experience with an existing three stage compressor in a transonic wind tunnel will be documented. The manner in which the theoretical properties manifest themselves in this non-ideal compressor will be described. A description of mistuning behaviors that can and cannot be accurately substantiated will be discussed. | | | |
| 14. SUBJECT TERMS Mistuning, Transonic wind tunnel compressor, Bladed disk | | 15. NUMBER OF PAGES 16 | |
| | | 16. PRICE CODE A03 | |
| 17. SECURITY CLASSIFICATION OF REPORT Unclassified | 18. SECURITY CLASSIFICATION OF THIS PAGE Unclassified | 19. SECURITY CLASSIFICATION OF ABSTRACT | 20. LIMITATION OF ABSTRACT |